Fibers and Polymers (2026) 27:2765–2782
https://doi.org/10.1007/s12221-026-01381-0

Online ISSN 1875-0052
Print ISSN 1229-9197

REGULAR ARTICLE

Boric Acid Influence on Ammonium Phytate Finish for Eco-Efficient Flame Retardancy of Cuprammonium Fabrics

Raphael P. Rosa[1] · **Giuseppe Rosace**[1,2,3]

Received: 6 October 2025 / Revised: 16 February 2026 / Accepted: 2 March 2026 / Published online: 25 March 2026

Abstract

Cuprammonium fabric is a regenerated cellulose fiber known for its silk-like luster appearance. However, due to its cellulose-based composition, the fabric is inherently flammable, limiting its application in many other areas. Therefore, the objective of this study was to evaluate two water-based finishes to improve fire performance: (i) APA, generated in situ from phytic acid and urea (ammonium phytate), and (ii) PAB, obtained by reacting boric acid with phytic acid and subsequently with urea. Compared to untreated fabric, APA- and PAB-treated samples exhibited self-extinguishing behavior and formed char layers during vertical flame tests, with char lengths of 35 mm and 33 mm, respectively, at a concentration of 400 g/L. Furthermore, thermogravimetric analysis in nitrogen showed an increase in char yield at 700 °C, from 0.23% (untreated) to 39.54% (APA) and 40.63% (PAB), indicating condensed-phase action (acid-catalyzed dehydration/char formation). Although the results demonstrated that the PAB-treated samples had no washing resistance, they exhibited better tear resistance and whiteness index compared to the APA-treated samples. Overall, the results show that both phosphate and nitrogen systems (with and without boron) significantly enhance the fire resistance of cuprammonium fabric by promoting protective char, while also revealing trade-offs in durability and appearance that require further improvement.

Keywords Cuprammonium fabric · Phytic acid · Boric acid · Flame retardancy · Synergism

1 Introduction

Textiles have been an integral part of human civilization, from simple clothing and shelter that protect us from harsh environmental conditions to the development of smart textiles capable of real-time monitoring of several types of health conditions, they have continuously evolved alongside humanity [1]. Textiles are utilized in various industries, including automotive, construction, aerospace, healthcare, and fashion, due to their versatility, durability, and ability to be tailored into diverse forms [2–4]. In 2024, the global market share of textiles was $ 2010.76 billion, a 10.04% increase from 2023 ($ 1837.27 billion), and it is expected to grow by 6.9% annually over the next eight years [5, 6]. However, the high demand for textiles also raises concerns about their environmental impact, especially with the rise of fast fashion, which primarily uses non-degradable synthetic fibers in its products [7]. Therefore, in the last years, sustainability has become a significant factor in textile production, driving research into biodegradable and recycled materials to reduce environmental impact while meeting the growing demand for innovative, high-performance textiles [8, 9].

Recently, regenerated cellulose has gained significant attention as an alternative method for producing natural fibers with properties comparable to those of synthetic fibers [10]. Its primary component is cellulose, the most abundant natural polymer on the planet, and by adjusting the regeneration parameters, the final product can take various shapes, such as powder, fibers, films, hydrogels, and spheres [11, 12]. Currently, there are two processes for producing regenerated cellulose: the derivatizing process and the direct dissolution (non-derivatizing) process. The primary difference

✉ Raphael P. Rosa
raphael.rosa@unibg.it

[1] Department of Engineering and Applied Sciences, University of Bergamo, Viale Marconi 5, 24044 Dalmine, BG, Italy

[2] Local CSGI (Inter-University Center for Colloid and Surface Science) Research Unit, Viale Marconi 5, 24044 Dalmine, BG, Italy

[3] Local INSTM (National Consortium of Materials Science and Technology) Research Unit, Viale Marconi 5, 24044 Dalmine, BG, Italy

between the two methods is that in the first process, cellulose is chemically modified before dissolution. In contrast, the second method involves directly dissolving the material in a solvent without any modification to regenerate fibers [13]. Even though both methods are similar, direct dissolution has shown some advantages over the derivatizing process, as it requires less energy and consumes fewer chemicals, and the solvents used can be reused and recycled [10].

Two widely known regenerated cellulose fibers manufactured through direct dissolution are Lyocell and cuprammonium fabric [14]. The first, Lyocell, is obtained by dissolving cellulose in N-methylmorpholine-N-oxide (NMMO). The dissolution-spinning cycle is completed within 3 to 4 h, and the resulting filaments combine high tenacity with excellent drape, enabling applications that range from apparel to conveyor belts, nonwovens and industrial filter media [15]. The second, cuprammonium fabric (also known as cuprammonium fibers and *cupro fibers*), is produced by dissolving cellulose in cuprammonium hydroxide. The process involves the use of several hazardous chemicals, like copper salts, sodium hydroxide, sulfuric acid, and ammonia, limiting its adoption worldwide [14]. Nevertheless, the Asahi Kasei Corporation in Japan claims that not only can it recover 99.9% of the copper used during the process, but its closed system also minimizes environmental impact by significantly reducing the release of harmful chemicals and wastewater into the environment [7, 16].

Compared to other regenerated fibers, cuprammonium fabric exhibits higher tensile strength, lower tensile elongation, good moisture absorption, and excellent chemical stability against alkalis and reducing agents [17, 18]. Its properties have been explored by several authors, for instance, Zhang et al. (2022), who coated cuprammonium fibers with graphene to enhance their conductivity properties. The treated fibers showed a significant increase in electrical conductivity, transforming from insulators to conductors [19]. Using the dipping–drying method, Cui et al. (2015) combined silver nanowires with *cuprammonium fibers* to create electrically conductive fabrics. According to the authors, the modified fibers exhibited excellent flexibility and conductivity, with the latter remaining stable even when the fabrics were subjected to stretching, shrinking, or bending. Furthermore, they observed that the fabric's electrical resistance increased accordingly with the strain percentage (%), where at 0%, strain the resistance was 0.0047 Ω, while at 190%, it was 0.0091 Ω [20]. D. Iqbal et al. (2025), on the other hand, used a functionalized cuprammonium fabric (comprising polyacrylonitrile and polyethene oxide) to remove dyes from water. The functionalized fabric achieved a 94%, 89.9%, and 87.4% efficiency for removing Congo red, metanil yellow, and methyl orange, respectively [21].

However, cuprammonium fabric has poor flame-retardant properties, which can limit its application in many areas. To address this drawback, a common approach is the functionalization of cellulose using flame retardants (FRs). These materials can change the combustion process by promoting char formation, reducing heat release, and slowing down flame propagation [22]. In recent years, significant progress has been made in developing halogen-free, eco-friendly, and bio-based flame-retardant systems for cellulose fibers [22].

Recent research has investigated bio-derived macromolecules as environmentally friendly and safe alternatives to traditional flame retardants. DNA, proteins, starches, and plant-based extracts (e.g., banana pseudostem sap and coconut shell) have all demonstrated the ability to improve the fire resistance of cellulose-rich substrates by promoting intumescence and char formation [23, 24]. The current focus is particularly on phytic acid (PA), a phosphorus-rich storage molecule found widely in seeds and grains that contains approximately 28 wt% phosphorus [25]. Due to its biocompatibility and high phosphorus content, PA has effectively enhanced the flame resistance of polyaniline-coated paper, poly(lactic acid) nonwoven fabrics, and ethylene–vinyl acetate copolymers through ion complexation or pad–dry–cure methods [23, 26, 27].

Another interesting type of flame retardant is boron-based, due to its non-toxicity, tastelessness, and colorlessness [28, 29]. Boron compounds, such as boric acid and borax, promote the formation of a protective glassy char layer during combustion, which acts as a barrier to isolate heat and oxygen, thereby slowing down the burning process [29]. Moreover, its acidity can also promote the formation of coke [30]. As a result, it has been used to impart flame-retardant properties to cellulose textiles for over two hundred years [31]. Unfortunately, boron-based FRs are easily hydrolyzed, which causes them to lose their flame resistance properties after a few laundering cycles [32, 33].

Nevertheless, some researchers have tried to improve boron-based FR efficiency and washing resistance by combining it with nitrogen and phosphorus FRs. For instance, Zhu W. et al. (2020) used boric acid, phytic acid, urea, pentaerythritol, and toluene to create a B/P/N flame-retardant formulation that significantly enhanced flame resistance and washing durability. According to their results, the PBN_30 samples (cotton fabrics treated with a 30 g/L FR solution) exhibited self-extinguishing behavior, with an average burned length of approximately 40 mm and a limiting oxygen index (LOI) above 45%. Moreover, the fabrics retained their FR behavior even after 50 washing cycles, where the burned length was 63 mm and the LOI value was 39%, only a 57.5% and 13.3% performance reduction, respectively [33]. Shi Y. et al. (2023), synthesized an eco-friendly flame retardant through the esterification of phosphorylated meglumine and boric acid, followed by its ammonification using urea. The authors evaluated different concentrations when treating the samples, where they varied from 50 g/L to 450 g/L

(increasing by a 100 g/L step). The burned length of the 50 g/L sample was approximately 81 mm, while the 450 g/L sample was 72.4 mm, resulting in a 10.6% difference. In the case of LOI, the 450 g/L samples showed a value of around 42%, which decreased to 30.5% after 30 washing cycles. According to the authors, this reduction may occur because the flame retardant did not properly cross-link onto the cotton fabric during the curing step, resulting in part of it being washed off after each washing cycle [29].

Although several phosphorus–nitrogen (P/N) and phosphorus–nitrogen–boron (P/N/B) flame-retardant (FR) systems (often based on ammonium phytate or related phosphate salts) have been reported for cellulosic based fabrics, their transferability to cuprammonium rayon is not self-evident, as finishing performance is strongly substrate-dependent. Variables such as fabric morphology (continuous fine filaments vs staple), aqueous solution uptake, and the number of hydroxyl groups available can lead to different add-on, deposition distribution, and, ultimately, different fire behavior after curing. Therefore, studying the FR effect on cuprammonium fabric directly is essential for obtaining accurate and dependable results. This work investigates the role of boron in the flame-retardant functionalization of cuprammonium fabric by testing whether its addition to a phytic acid/urea/dicyandiamide P/N system enhances thermal stability and flame resistance. To achieve this, a one-pot aqueous B/P/N formulation consisting of boric acid, phytic acid, urea, and dicyandiamide was prepared and compared against a boron-free analogue made under identical conditions. The properties of the functionalized fabrics were investigated using several characterization techniques, including FTIR, Raman, SEM, TGA, vertical combustion, and tear resistance. To the best of our knowledge, this is the first controlled comparison of boron-containing and boron-free systems on cuprammonium fabric. By making these such modifications, this study aims to expand the applicability of cuprammonium textiles in technical and protective applications.

2 Experimental

2.1 Materials

Cuprammonium fabric with a mass per unit area of 103 g·m^{-2} and 0.21 mm thickness was generously provided by the Asahi Kasei Group (Nobeoka, Miyazaki Prefecture, Japan).

N, N-Dimethylformamide (DMF), phytic acid 50% (w/w) in water solution, anhydrous ethanol (99%), urea flakes (99.0–100.5%), acetic acid (99%), and boric acid powder (≥ 99.5%) were purchased from Merck (Milan, Italy). Dicyanamide (99%) was supplied by Alfa Aesar (Segrate, Italy). All chemicals and reagents were used directly without further purification.

2.2 Synthesis of Ammonium Phytate (APA) and Boric Ammonium Phytate (PAB)

The syntheses of both ammonium phytate (APA) and boric ammonium phytate (PAB) were modified from the works of Zhu et al. (2022), Ma et al. (2021), and Shi et al. (2023) [29, 34, 35]. In a 250-mL three-necked flask, equipped with a magnetic stirrer and a reflux condenser, 40 g of phytic acid (0.04 mols) and 10.49 g of boric acid (0.17 mols) were added. The reaction mixture was stirred and heated in an oil bath at 130 °C for 8 h under reflux and then cooled down to 30 °C. Once at 30 °C, 15.28 g of urea (0.25 mols) was added. The reaction was then carried out under stirring for a total of 4 h: the first 2 h at 110 °C, followed by an increase to 130 °C for the last 2 h. Finally, a light-brown viscous product with a complex viscosity of 120.98 ± 0.99 Pa s was obtained (Scheme 1).

Moreover, to evaluate the impact of boric acid on flame-retardant performance, a parallel formulation was produced without its addition, denominated as APA. For this, 40 g of phytic acid (PA) was mixed directly with 10.92 g of urea, following a 1:6 PA/urea molar ratio, using the same temperature and time as before. After the reaction was over, DMF was used to separate ammonium phytate (APA) from the unreacted material. Finally, the APA was washed 3 times using anhydrous ethanol and put under vacuum overnight to remove the DMF. The final product was a light-brown solid. Scheme 2 shows the reaction process.

Six flame-retardant solutions were prepared by mixing varying concentrations of APA or PAB with water and dicyandiamide at a 1:6 molar ratio. First, PAB or APA was transferred to a 250-mL beaker, and water was added until the appropriate concentration was achieved. Then, the solution was stirred continuously, and using a pH meter, acetic acid was added dropwise until the solution reached a pH of 5, to enhance the interaction between the cellulose and dicyandiamide. Subsequently, dicyandiamide was added in the required amount to achieve a 1:6 ratio, and the mixture was heated to 70 °C and stirred until complete dissolution was achieved. The samples were classified by primary active material and concentration, using the prefixes "APA_" or "PAB_" for ammonium phytate and boric ammonium phytate, respectively, and the suffixes "_150," "_200," and "_400" indicating solution concentrations of 150 g/L, 200 g/L, and 400 g/L.

2.3 Flame-Retardant Treatment of Cuprammonium Fabric

Flame-retardant cuprammonium fabric was fabricated using the following steps. First, the fabric was cut into A4 sizes

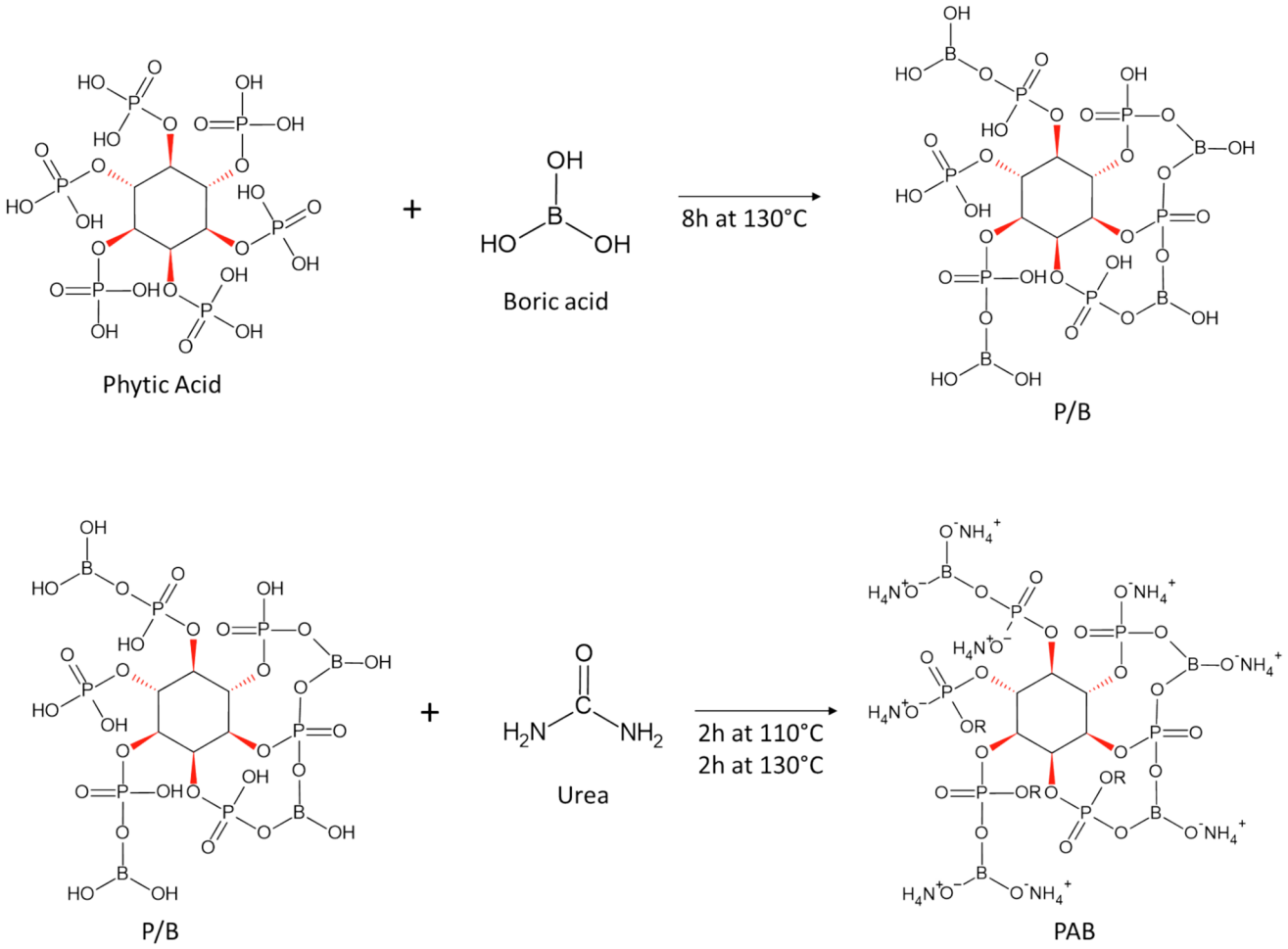

Scheme 1 Synthesis of boric ammonium phytate (PAB). The R can be a –H, –OH, or a NH_4^+ group

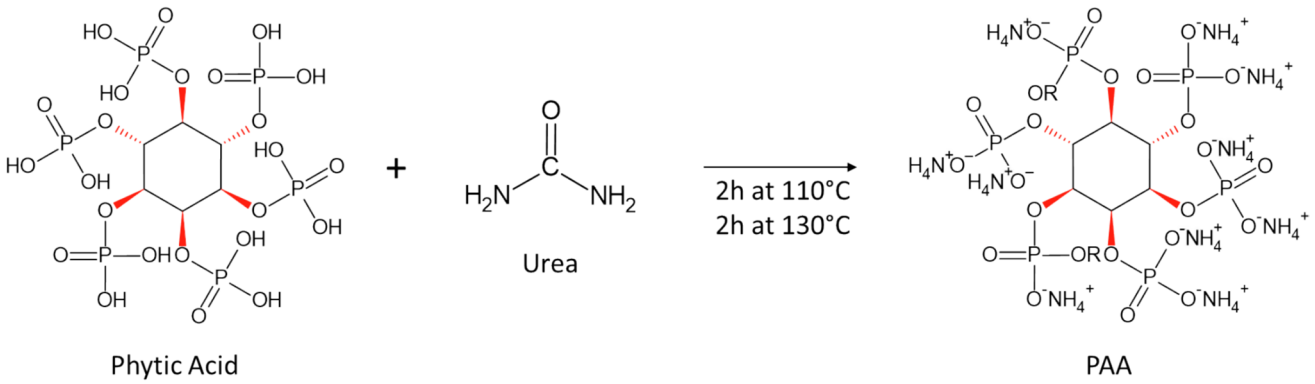

Scheme 2 Synthesis of ammonium phytate (APA). The R can be a –H, –OH, or a NH_4^+ group

(20 cm weft × 30 cm warp), with the long edge aligned parallel to the selvage. Each fabric was weighed three times to obtain an accurate dry mass. Then, using a two-roll laboratory padder (Werner Mathis, Zurich, Switzerland) with a nip pressure of 2 kg·cm^{-2}, the cut fabrics were impregnated separately three times with each flame-retardant formulation, either including or excluding boric acid. Immediately after padding, the wet specimens were weighed three times to determine the wet pickup. Then, they were dried at 80 °C for 5 min and cured in a gravity convection oven at 180 °C

for 1 min. The latter conditions were selected to avoid prolonged exposure at elevated temperatures, as longer curing times can lead to cellulose structural degradation [36, 37].

Before all experiments, the samples were conditioned under standard atmospheric pressure at 65 ± 4% relative humidity (RH) and 20 ± 2 °C for at least 24 h. The add-on values A (%) were calculated as reported in Eq. 1.

$$A(\%) = \frac{\left(W_{\text{treated}} - W_{\text{untreated}}\right)}{W_{\text{untreated}}} \times 100 \quad (1)$$

where ($W_{\text{untreated}}$) and (W_{treated}) represent the dry mass of the specimen before and after finishing, curing, and conditioning, respectively.

2.4 Washing Procedure

The functionalized cuprammonium samples underwent 1 to 5 washing cycles following the ISO 105-C10:2006 standard method [38]. The samples were immersed in a soap solution with a concentration of 5 g/L, preheated to 40 °C, and maintained at a liquor ratio of 50:1 for 30 min in a Mathis Labomat (Werner Mathis, Zurich, Switzerland). No surfactants were included to prevent their potential adsorption onto the fabrics, which could complicate the interpretation of the FTIR spectra. After each laundering cycle, washed samples were dried at 105 ± 3 °C in a forced-air oven until constant mass was reached (≤ 0.1 mg change in two successive weighting, typically 90 min for the fabric used), cooled to room temperature in a desiccator over fresh silica gel, and then weighed to the nearest 0.1 mg. The weight loss of fabric after washing cycles (WLW, wt%) concerning the unwashed samples was calculated according to Eq. 2.

$$\text{WLW}\% = \frac{W_{\text{treated}} - W_n}{W_{\text{treated}}} \times 100 \quad (2)$$

where (W_{treated}) and (W_{n}) denote the dry mass of the treated fabrics before and after n wash cycles, respectively, according to the ISO 105-C10:2006 [38]. The reported values represent the average of three different weighs on each sample.

2.5 Characterization

Several characterization methods were employed to investigate various properties of both treated and untreated samples. Morphological analyses were performed using a scanning electron microscope (SEM, Phenom ProX G6 Desktop SEM, Thermo Fisher Scientific, Italy). The microscope was equipped with an energy-dispersive X-ray spectrometer (EDS), which analyzed the distribution of chemical elements on the surfaces of treated and untreated cuprammonium fabric, operating at a voltage of 15 kV. Each sample was placed on aluminum sample holders through a graphite adhesive.

CIE whiteness index between treated and untreated textile samples, as well as before and after washing cycles, was measured using a Datacolor Spectro 700 spectrophotometer (Datacolor, Italy) following the ISO 105–102:1997 and ISO 105-J03:2009 [39, 40]. All measurements were taken using a USAV 9-mm aperture under D65 illumination with a 10° standard observer, and the fabrics were folded four times to ensure that the image capture by the instrument was from the textile. The specular component was included for the CIE whiteness index. An average of three measurements was recorded for each sample. The whiteness index (W_{CIE}) was calculated using Eq. 3, where X (related to red/green sensibility), Y (the luminance), and Z (the blue sensibility) are the tristimulus values and x_n and y_n are the chromaticity coordinates for the diffuser under D65.

$$W_{\text{CIE}} = Y + 800 \times \left(x_n - \frac{X}{X+Y+Z}\right) + 1700 \times \left(y_n - \frac{Y}{X+Y+Z}\right) \quad (3)$$

To compare the chemical surface modifications introduced by the coatings, FTIR spectra of both treated and untreated samples were acquired using a Thermo Avatar 370 spectrometer (Thermo Nicolet Corp., USA), equipped with an attenuated total reflection (ATR) diamond crystal accessory. Three replicate spectra were recorded for each sample in absorbance mode, spanning the range of 4000 to 700 cm^{-1}, based on 32 scans averaged at a resolution of 4 cm^{-1}. Average spectra of textiles were normalized at 840 cm^{-1} bandwidths (C–H deformation), which is in a region where the finishing is absent. The spectra were analyzed using Omnic v 9.2 and processed using RStudio with Origin v 8.0.

Raman spectroscopy was performed over the spectral range of 50–5000 cm^{-1} using an XploRA Plus Raman spectrometer (HORIBA Scientific, Italy) integrated with an Olympus confocal microscope, equipped with a 600 groove/mm diffraction grating. The excitation source was a 532-nm laser focused on the sample through a 100× objective lens (numerical aperture of 0.9), delivering a laser power of 100 mW at the sample surface. The acquisition time for each spectrum was set to 10 s, and 5 accumulations were taken. Each sample underwent three measurement repetitions to ensure reproducibility. A baseline correction was applied to each Raman spectrum, followed by min–max normalization using RStudio. The area under the curve of each spectrum was calculated using the Gaussian model provided in Origin v8.0 software.

Rheological measurements of the PAB flame-retardant solution were performed using a Discovery HR10 rheometer (TA Instruments) with a 20-mm flat geometry at a constant temperature of 25 °C. The complex viscosity was determined from a ramp amplitude test where γ ranged from 0.01 to 100% and $\omega = 10$ rad/s.

Thermal and thermo-oxidative stability analyses of the flame-retardant finishing fabrics were carried out using a Discovery TGA550 (TA Instruments), where the temperature ramp was set from 25 to 800 °C at a heating rate of 10 °C min^{-1} with a flow rate of 90 ml min^{-1}. The analyses were conducted under nitrogen atmospheres. The experimental error was ± 0.5% on the weight and ± 1 °C on the temperature. Based on the analysis results, the temperature at 5% mass loss (T_5%), the onset temperatures of the main and secondary mass-loss events (Ta_{onset} and Tb_{onset}), and the temperatures at the maximum mass-loss rates for the main and secondary events (Ta_{max} and Tb_{max}) were calculated.

Thermogravimetric and infrared analysis (TG-FTIR) was performed using a Discovery TGA550 thermogravimetric analyzer coupled with a Thermo Avatar 370 infrared spectrometer (TG-FTIR) to analyze the thermal decomposition and evolved gases of the sample. A REDshift evolved gas analyzer (REDshift, Italy) interface was employed to connect the TGA with the FTIR. The analysis was conducted under a nitrogen atmosphere with a flow rate of 90 mL·min^{-1}. The temperature ramp was set from 30 to 800 °C with a heating rate of 10 °C·min^{-1}. The decomposed volatiles were transferred through a heated line maintained at 250 °C at a flow rate of 90 mL·min^{-1} into the FTIR gas cell. Spectra were recorded in the wavelength range of 650–4000 cm^{-1}. The obtained spectra series were analyzed using Omnic v 9.2.

The fabric vertical burning flammability test was conducted in accordance with ASTM D6413–08, using a sample size of 76 mm × 300 mm and an ignition time of 12 s [41].

Mechanical tests were performed using an Elmendorf tear test following the ASTM D1424-21 standard. The method measures the tear resistance of the material by quantifying the force required to propagate a tear [42].

The flexural rigidity of the treated and untreated samples was evaluated according to ASTM D1388-2018 [43]. For each sample, a fabric strip of 152.4 mm in length and 25.4 mm in width was cut. The test was performed 5 times for each sample, and the bending length (C) and flexural rigidity (G) of the sample were determined using Eqs. 4 and 5, respectively.

$$C = \frac{l}{2} \tag{4}$$

$$G = W \times C^3 \tag{5}$$

where W represents the fabric's weight (mg/cm^2), C is the bending length (cm), and l is the sample's hanging length (cm).

3 Results and Discussion

3.1 Surface Morphology and Chemical Characterization

Table 1 summarizes the liquor retention (wet pickup) recorded during the pad–dry–cure step and the final mass gain (add-on) of the treated cuprammonium fabrics. For both APA- and PAB-treated samples, both wet pickup and add-on increased accordingly with concentration, suggesting an efficient uptake and retention of the FR. Moreover, PAB_400 showed the highest wet pickup and add-on, indicating a stronger interaction with the cuprammonium structure and a more efficient deposition.

The absorption peaks of both the materials used in the flame-retardant synthesis, and the resulting products (APA and PAB) are shown in Fig. 1. For both APA and PAB, the spectral bands from 3600 cm^{-1} to 3200 cm^{-1} correspond to the H–O–H bending, indicating the slight presence of water. The presence of peaks at 3200 cm^{-1} 1150 cm^{-1} and 1625 cm^{-1} in both APA and PAB is related to the N–H stretching vibrations and bending deformation, respectively [44]. The peak around 1450 cm^{-1} can be the C–N or B–O–C stretching vibration, while the peak at 2850 cm^{-1} is attributed to C–H stretching vibrations [45]. In the case of the phosphorous groups, the peak at 1630 cm^{-1} corresponds to the P=O stretching vibration, the weak absorption around 910 cm^{-1} is assigned to P–O–H bending, and the peak at 1040 cm^{-1} is associated with P–O–C stretching vibrations [46, 47].

The spectra of the untreated and treated cuprammonium samples are shown in Fig. 2. Regarding the untreated cuprammonium fabric, its infrared spectrum is essentially the same as that of other regenerated cellulose [48]. The presence of a long peak around 3700–3400 cm^{-1} can be attributed to the O–H stretching from the hydroxyl groups (including intra- and intermolecular hydrogen bonds) in the cellulose backbone. Meanwhile, the peak near 2900 cm^{-1} can be attributed to aliphatic C–H stretching. A band near 1630–1650 cm^{-1} is assigned to H–O–H bending of absorbed

Table 1 Wet pickup (%) and add-on (%) of PAB- and APA-treated samples

Sample code	Wet pickup (%)	Add-on (%)
APA_150	86.86 ± 0.004	13.11 ± 0.068
APA_200	90.64 ± 0.016	18.66 ± 0.002
APA_400	92.71 ± 0.037	27.44 ± 0.001
PAB_150	89.56 ± 0.137	13.95 ± 0.023
PAB_200	87.13 ± 0.023	15.56 ± 0.004
PAB_400	105.05 ± 0.002	31.93 ± 0.015

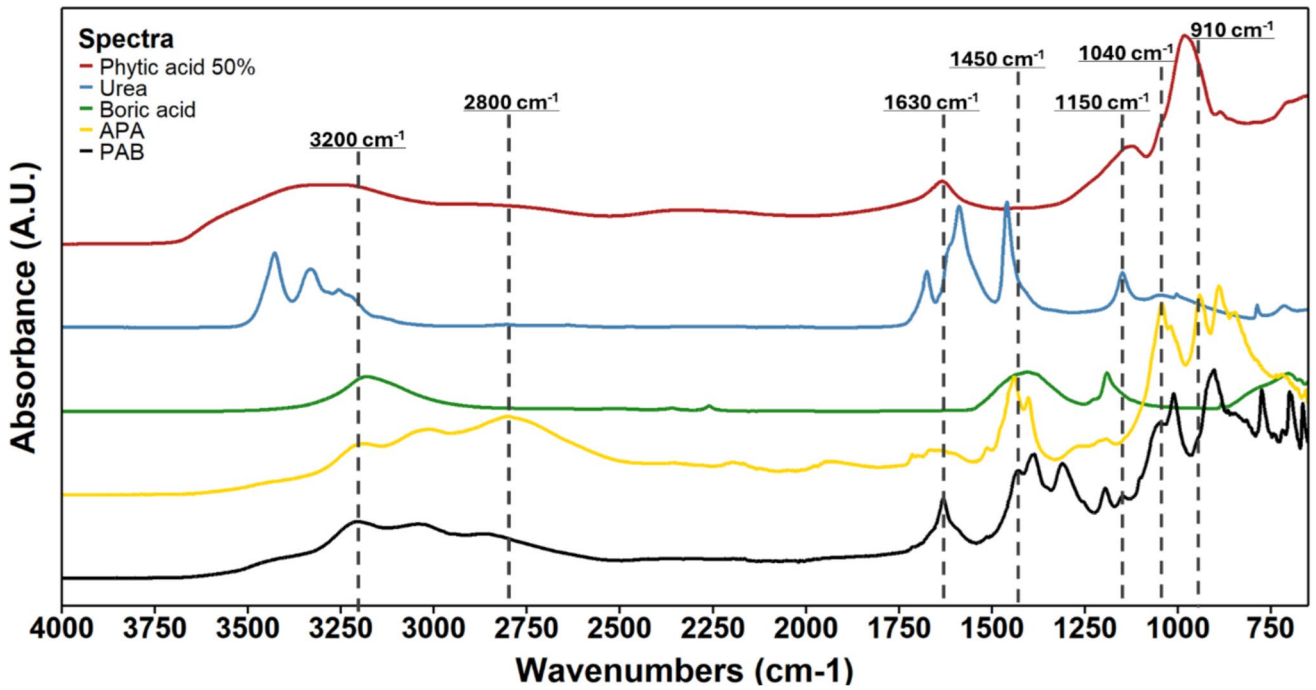

Fig. 1 FTIR spectra of the raw materials used for the FR reaction and the final products (APA and PAB). The FTIR spectra of APA (solid) and PAB (viscous) were acquired from purified samples following the purification process

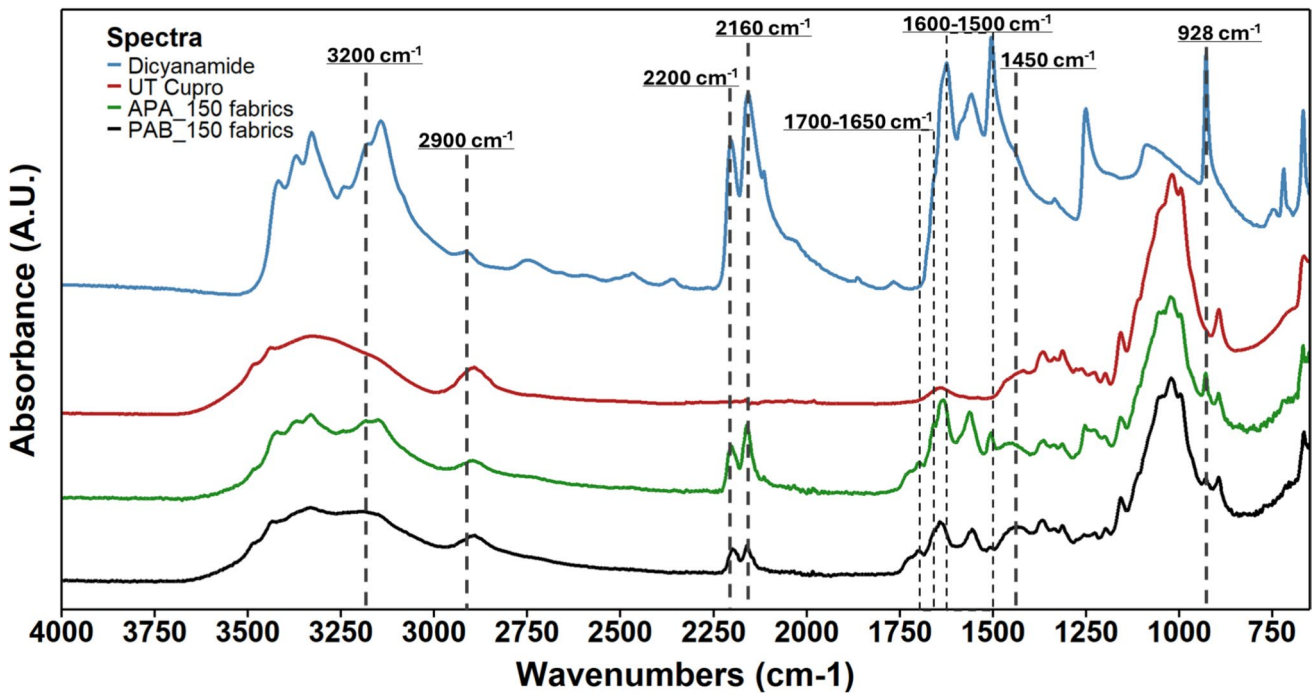

Fig. 2 FTIR spectra of dicyanamide, untreated cuprammonium fabric, APA_150 fabric and PAB_150 fabric (both were functionalized using a 150 g/L solution). Increasing the FR concentration to 200 g/L and 400 g/L had no significant change in the FTIR spectra

water. The peak around 1430 cm^{-1} results from asymmetric CH_2 bending in cellulose, and it is often referred to as the "crystallinity band" due to its correlation with the degree of crystallinity in the samples. The peaks near 1365 cm^{-1} and 1315 cm^{-1} are related to the C–OH and C–H bending, respectively. Furthermore, the peak at 1285 cm^{-1} is related

to CH_2 scissoring, while the peak at around 1050 cm^{-1} is due to the C–O stretching. Finally, a small band around 895–900 cm^{-1} corresponds to the β-(1 → 4) glycosidic ring vibration [48].

Upon functionalization with APA_150 and PAB_150 in the presence of dicyanamide, a clear change in the spectra of the untreated cuprammonium is observed. Both APA_150 and PAB_150 functionalized textiles showed new peaks at 2203–2163 cm^{-1}, which are associated with the asymmetric stretching vibration of the N=C=N group, possibly coming from the dicyanamide. Furthermore, the peaks at around 1500–1600 cm^{-1} and at 928 cm^{-1} are likely related to the asymmetric stretching vibration of the N–C–N group and the NH_2 skeletal vibration, respectively [49]. The peaks at around 1650–1700 cm^{-1} can correspond to either the P=O stretching vibration or N–H bending deformation. Overall, the FTIR results demonstrated that both APA and PAB were successfully incorporated into the cuprammonium fabric structure.

The surface morphological characteristics of untreated and treated cuprammonium samples with different concentrations of APA and PAB are shown in the SEM images in Figs. 3 and 4, respectively.

The untreated cuprammonium fabric at 1000x (Fig. 3a) exhibits a smooth and clean fiber surface with no visible fiber damage or any type of coating. However, it is possible to see a few small particles across the fabric. These small particles varied in size, ranging from approximately 10 µm to 1 µm (as shown in Fig. 3a'). Additionally, upon performing an EDX analysis, the particles were composed mainly of C (42.32%), O (12.39%), Cu (33.76%), and Zn (11.53%). These particles are most likely to be residues from the textile fabrication process that were not completely removed.

After functionalization with APA, the fabric started to exhibit the presence of larger particles and coating structures that became progressively denser and more uniform on the surface as the FR concentration increased (Fig. 4a, b, and c). The presence of the coating material was further confirmed by EDS analysis, as shown in Table 1, where the phosphorus (P) and nitrogen (N) content increased in proportion to the FR concentration. Compared to the APA functionalized samples, the fabrics treated with PAB, which contained boron, exhibited a more textured and granular surface (Fig. 4a', b', and c'). Moreover, as PAB concentration increased, the coating appeared more continuous and compact, suggesting improved deposition and interaction between the FR and the fabric. Finally, similar to the samples treated with APA, the EDS analysis (Table 2) showed that increasing the concentration of the FR leads to a higher amount of P, N, and B.

However, as shown in Table 2, both APA- and PAB-treated samples started to lose part of their FR elements after each washing cycle, with the latter exhibiting a more pronounced loss. As observed, the nitrogen content was most affected after the first washing cycle, whereas the phosphorus content remained relatively stable. The reason is likely due to the excess of dicyandiamide in the formulation.

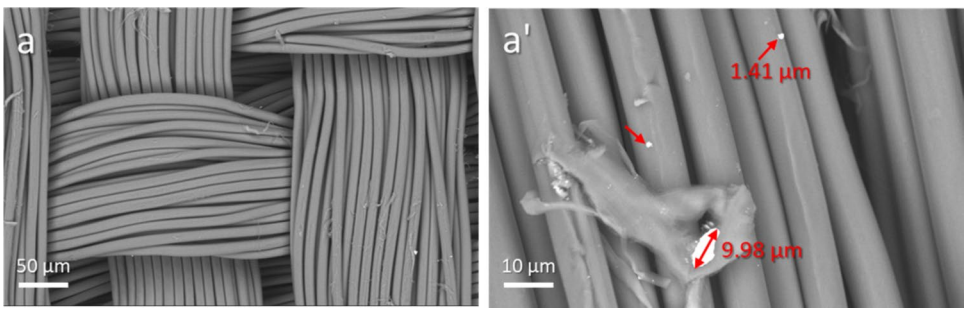

Fig. 3 SEM images of untreated cuprammonium fabric at different magnifications. Image **a** is at 1000 × and **a'** is at 5000x

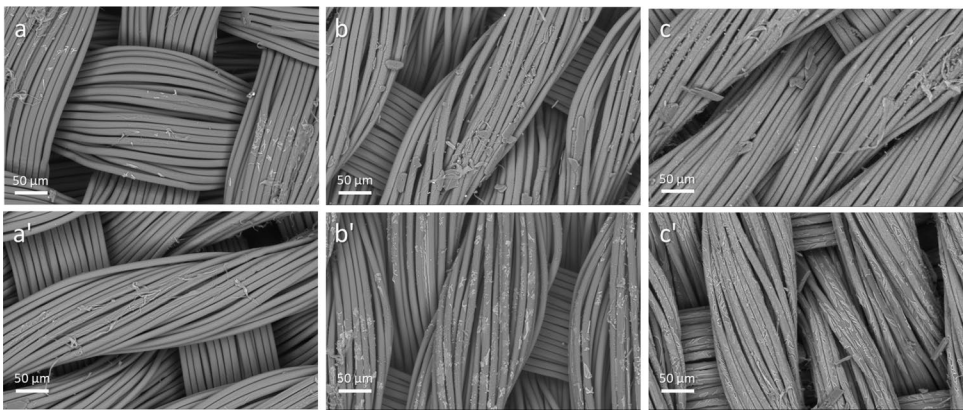

Fig. 4 SEM images of treated cuprammonium fabrics with APA and PAB at increasing concentrations (following the alphabetical order 150 g/L, 200 g/L, and 400 g/L). The images a, b, and c are related to APA-treated fabric, whereas the images a', b', and c' correspond to PAB-treated fabric

Table 2 EDS atomic concentration analysis of untreated, unwashed treated, and washed treated cuprammonium fabrics

Sample code	Number of washes	C	O	N	P	B
UT cuprammonium fabric	UW	50.64	49.36	–	–	–
APA_150	UW	32.58	45.86	20.29	1.27	–
	1	41.13	48.45	9.78	0.64	–
	3	42.82	47.86	8.72	0.60	–
	5*	41.34	48.56	9.3	0.55	–
APA_200	UW	26.53	32.27	40.60	0.60	–
	1	39.62	47.51	12.13	0.74	–
	3	43.79	47.72	8.17	0.32	–
	5	43.00	47.24	9.49	0.27	–
APA_400	UW	25.70	40.41	32.05	1.84	–
	1	34.39	46.54	17.33	1.74	–
	3	32.22	45.17	20.63	1.98	–
	5	35.73	48.02	14.80	1.45	–
PAB_150	UW	31.20	48.50	16.80	1.40	2.10
	1	45.73	44.25	9.61	0.41	–
	3	49.08	43.86	6.66	0.40	–
	5	50.63	49.37	–	–	–
PAB_200	UW	23.50	45.10	26.90	2.70	1.80
	1	49.34	42.18	8.03	0.45	–
	3	49.82	48.12	1.7	0.36	–
	5	48.36	48.93	2.71	–	–
PAB_400	UW	23.45	46.42	25.08	2.58	2.47
	1	42.56	44.48	10.19	0.45	2.32
	3	42.46	44.41	12.68	0.45	–
	5	42.83	44.34	12.38	0.45	–

*A small amount of calcium (0.25%) was detected, which probably came from the soap during washing

Furthermore, the hydrophilic nature of boron made it easier for phosphorus and nitrogen groups to be washed off during repeated washing cycles [34].

3.2 Whiteness Index Analysis

The influence of APA and PAB on the whiteness and color of cuprammonium fabric is described in Fig. 5a-d. The untreated cuprammonium fabric has a whiteness index of 52.862 ± 1.348. As described in Fig. 5a, the application of APA resulted in a drastic reduction in fabric whiteness, with the degree of reduction directly correlated to the concentration of APA. The phytic acid used in the synthesis of both APA and PAB flame retardants initially exhibited a light-brown color, which turned into a darker brownish solution following its reaction with urea at 130 °C. Consequently, when the fabrics were treated with flame-retardant solutions, they acquired a visibly darker tone. This behavior was also observed when phytic acid was used to improve the flame retardancy of wool [50]. Furthermore, during the curing process, the fabrics were exposed to 180 °C for 1 min. During this time, the cellulose naturally underwent thermal yellowing, which may have further contributed to the reduction in whiteness [51].

On the other hand, the cuprammonium fabric treated with PAB exhibited a smaller reduction in whiteness. This effect can be due to the multifunctional role of boric acid. In addition to acting as a stabilizing agent that forms reversible covalent bonds (borate esters) between the hydroxyl groups of cellulose and phytic acid, boric acid may also contribute to optical preservation through catalytic bleaching mechanisms [52, 53]. Furthermore, the presence of boron in other FR systems has been shown to slow down fabric yellowing during high-temperature curing [54].

The whiteness index was also measured after 1, 3, and 5 washing cycles, as shown by Fig. 5b-d. After one cycle, the APA and PAB whiteness index increased on average by 78.72% and 188.17%, respectively, whereas after five cycles, the increases were 102.40% and 248.57%, respectively. The rise in the whiteness index can be attributed to the partial removal of FR from the fabrics during the multiple washing process.

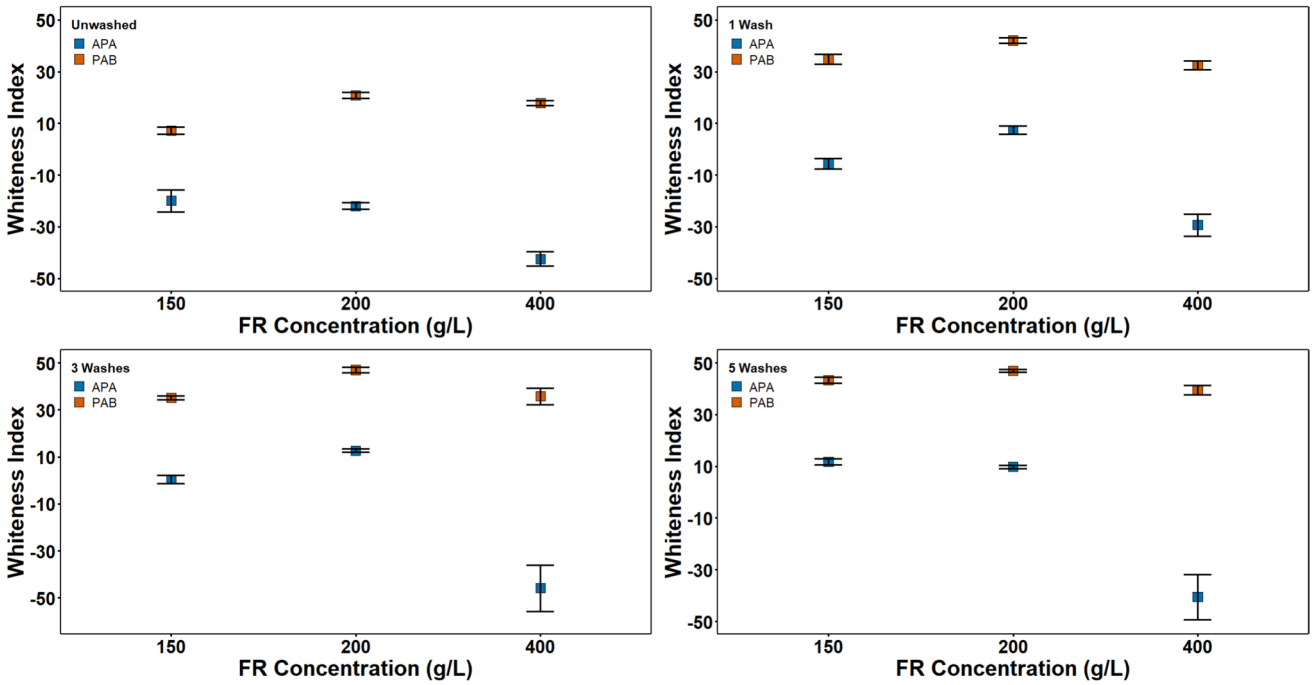

Fig. 5 Whiteness index of: **a** unwashed samples and after **b** 1, **c** 3, and **d** 5 washing cycles

3.3 Flame-Retardant Performance

Vertical flame tests were carried out to evaluate the flame-retardant performance of the functionalized cuprammonium fabrics before and after 1, 3, and 5 washing cycles. This is a standard test for assessing the flammability behavior of textiles, used in many previous works [32, 55]. As shown in Fig. 6, untreated cuprammonium fabric burns completely, leaving no char residue behind. On the other hand, all treated samples demonstrated flame-retardant capabilities, with an average char length of 48 mm for the APA samples and 42.6 mm for the PAB samples (Table 3). Moreover, as expected, increasing the concentration of the flame retardant resulted in improved fire resistance, as shown by the shorter char length in Fig. 6. Unfortunately, a gradual decline in flame-retardant performance was observed with increasing washing cycles. This was particularly pronounced for the PAB-treated samples and those with a lower FR concentration (150 g/L). All the PAB samples demonstrated a lower retention of FR in their structure and significantly lower performance when compared to the APA samples at the same concentration. This reduction can be attributed to the hydrolysis of the boron groups in the PAB-treated samples during laundering, resulting in a greater loss of N, P, and B elements [29, 32].

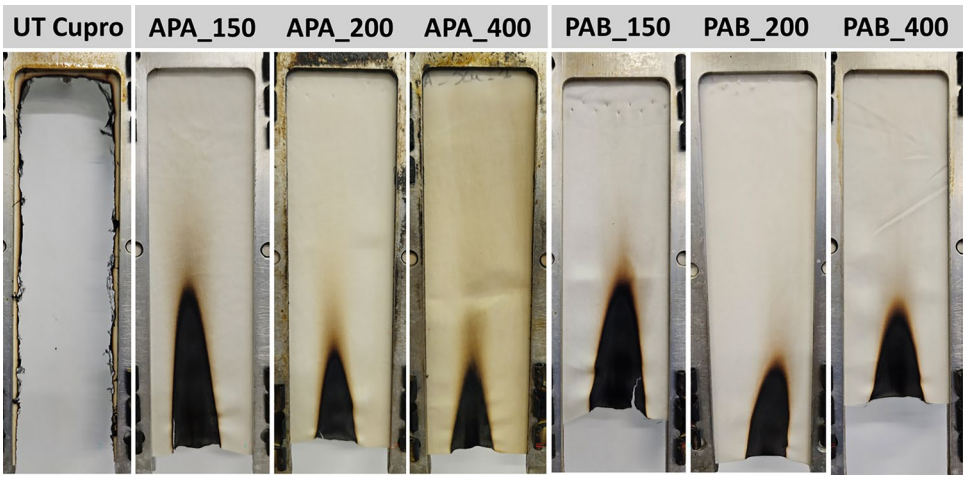

Fig. 6 Vertical flammability test of untreated and treated samples without washing

Table 3 Char length of PAB- and APA-treated and untreated samples after 0, 1, 3, and 5 washing cycles

Sample codes	Char length (mm)			
	UW	1 washing cycle	3 washing cycles	5 washing cycles
UT cuprammonium fabric	–	–	–	–
APA_150	67	All char	–	–
APA_200	42	All char	–	–
APA_400	35	45	47	46
PAB_150	50	All char	–	–
PAB_200	45	All char	–	–
PAB_400	33	All char	All char	–

Notably, only one of the formulations (APA_400) retained significant flame resistance after five washing cycles, maintaining self-extinguishing behavior and limiting char propagation. A complete overview of the flammability results is summarized in Table 3.

The char residue after vertical flame test of the untreated and treated samples (both APA and PAB) was also examined by Raman spectroscopy, as shown in Fig. 7. The characteristic D and G bands, associated with amorphous carbon and graphitic carbon, respectively, were positioned at approximately 1350 cm^{-1} and 1580 cm^{-1}. The I_D/I_G ratio was determined by calculating the ratio of the areas under the D and G peaks, where a lower I_D/I_G ratio indicates a higher material graphitization. This suggests that the material was able to better isolate oxygen and heat during combustion by forming char, thus improving its flame-retardant properties [56, 57]. The I_D/I_G ratio of untreated cuprammonium fabrics was 6.48, while those treated with APA and PAB were on average, 3.62 and 3.81, respectively. Furthermore, the difference between the two treatments is minimal, indicating no significant variation. Nevertheless, the overall reduction in the I_D/I_G value demonstrates that both treatments were able to improve char formation.

Finally, SEM analysis was carried out to examine the cuprammonium fabric's morphology after the vertical flame test. As shown in Fig. 8, the APA-treated samples, particularly those treated at 400 g/L (APA_400), retain a compact fibrous structure, surrounded by a continuous layer of glassy carbon where only superficial burning is visible. These findings support a flame-retardant mechanism based on the P/N effect, where the phosphorus units promote dehydration and carbonization in the condensed phase, while nitrogen functionalities contribute to gas-phase radical quenching, collectively blocking flame propagation [58]. On the other hand, the PAB-treated samples showed an uniform distribution of char formation across the fabric, with the boron acting as a surface sealing, reducing the rate of combustion [34, 59].

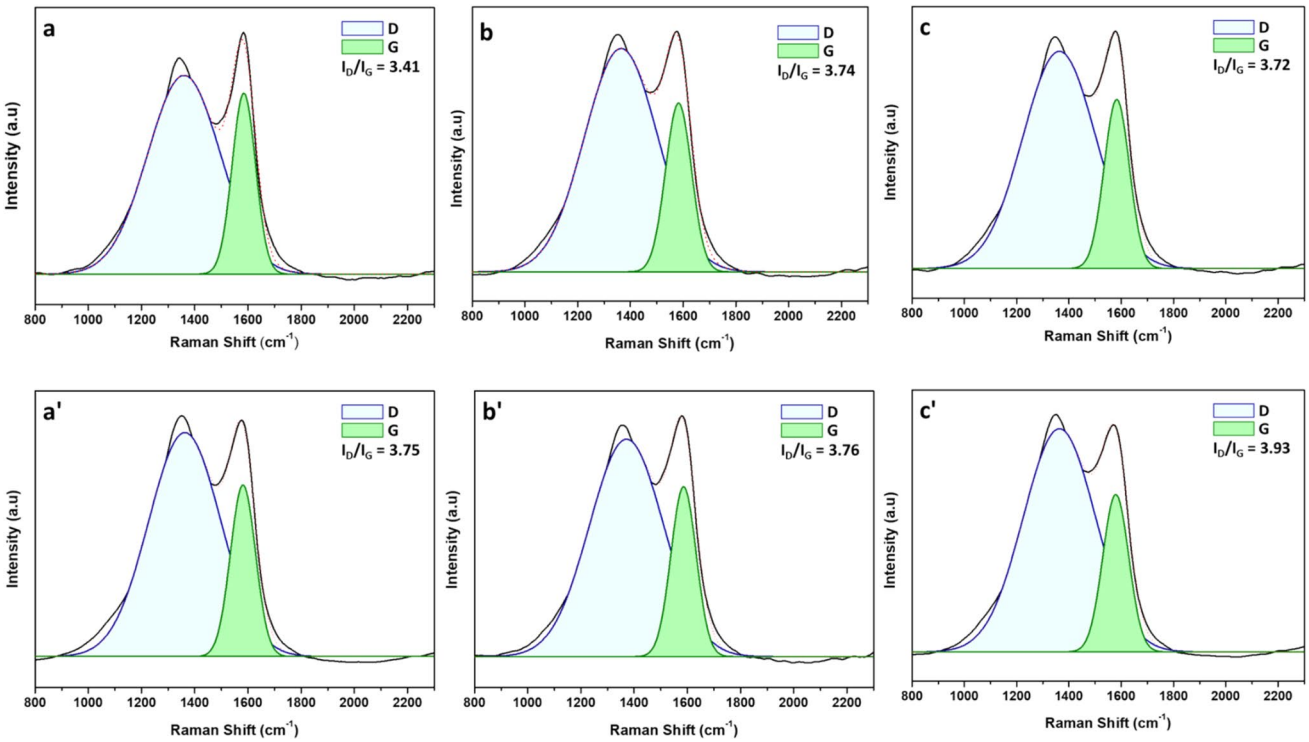

Fig. 7 Raman spectra of char residues of **a** APA_150, **b** APA_200, **c** APA_400, **a'** PAB_150, **b'** PAB_200, and **c'** PAB_400

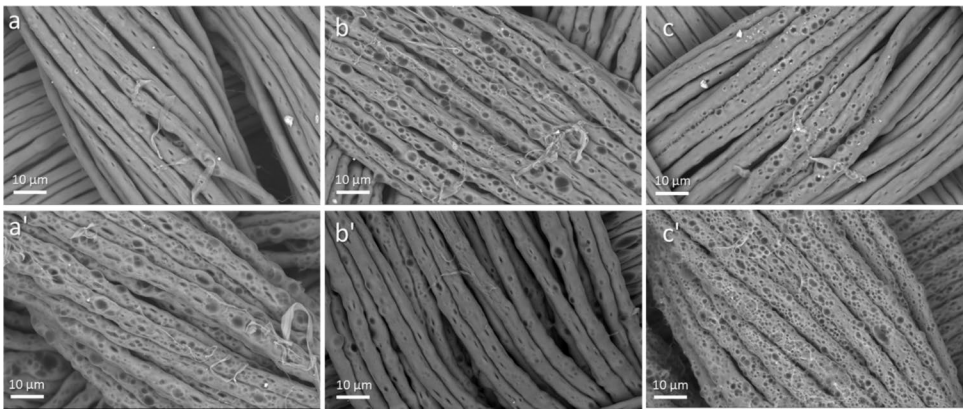

Fig. 8 SEM images of unwashed treated cuprammonium fabrics after burning: **a** APA_150, **b** APA_200, **c** APA_400, **a'** PAB_150, **b'** PAB_200, and **c'** PAB_400. All images were taken with a 2500× magnification

3.4 Thermogravimetric Analyses

Thermogravimetric analyses in nitrogen were performed to evaluate the thermal stability of the untreated and treated fibers before and after 1, 3, and 5 washing cycles. A summary of the results is shown in Table 4 and Fig. 9.

As shown by Table 4, all treated samples (UW APA and UW PAB series) exhibit significantly improved thermal stability compared to the untreated cuprammonium fabric. This is evident from the higher T_5% values, indicating that the treated materials began to lose their masses at higher temperatures. Moreover, the residue at T_{max1} and 700 °C is substantially greater for treated samples, suggesting

Table 4 Thermogravimetric data for unwashed and washed treated samples at increasing concentrations

Sample code	Number of washes	$T_{5\%}$ [ºC]	Ta_{onset} [°C]	Ta_{max}* [°C]	Tb_{onset} [°C]	Tb_{max}* [°C]	Residue at 700 °C [%]
UT cuprammonium fabric	UW	115.29	275.12	353.10	–	–	0.23
APA_150	UW	171.82	225.01	261.21	265.72	275.00	29.00
	1	237.47	240.74	260.80	272.74	286.90	31.25
	3	239.28	239.95	259.61	268.16	286.60	33.13
	5	116.56	244.23	266.17	270.11	290.51	21.09
APA_200	UW	194.72	230.51	258.85	266.19	277.21	36.42
	1	214.47	242.53	265.61	274.37	288.31	33.48
	3	107.95	265.65	307.80	–	–	15.91
	5	79.82	265.45	309.20	–	–	7.91
APA_400	UW	186.25	220.05	235.19	247.01	260.10	39.54
	1	183.91	218.00	249.80	260.02	275.60	31.32
	3	215.55	226.81	250.80	258.31	272.80	38.64
	5	231.18	231.51	258.20	268.79	279.91	37.50
PAB_150	UW	137.21	249.29	269.91	275.97	286.80	32.74
	1	215.18	267.00	308.90	–	–	11.36
	3	253.06	249.43	270.84	278.88	298.20	26.757
	5	291.74	293.50	339.80	–	–	1.36
PAB_200	UW	159.32	246.07	272.61	275.02	287.49	37.08
	1	237.27	261.00	304.01	–	–	21.99
	3	108.16	270.84	311.6	–	–	15.36
	5	69.33	308.30	345.81	–	–	0.11
PAB_400	UW	125.41	237.66	264.29	281.50	290.60	40.63
	1	252.47	250.02	271.77	278.85	298.00	26.40
	3	214.98	236.10	260.02	270.58	291.40	24.94
	5	255.82	250.9	275.11	286.94	300.60	25.79

*From the derivative curves

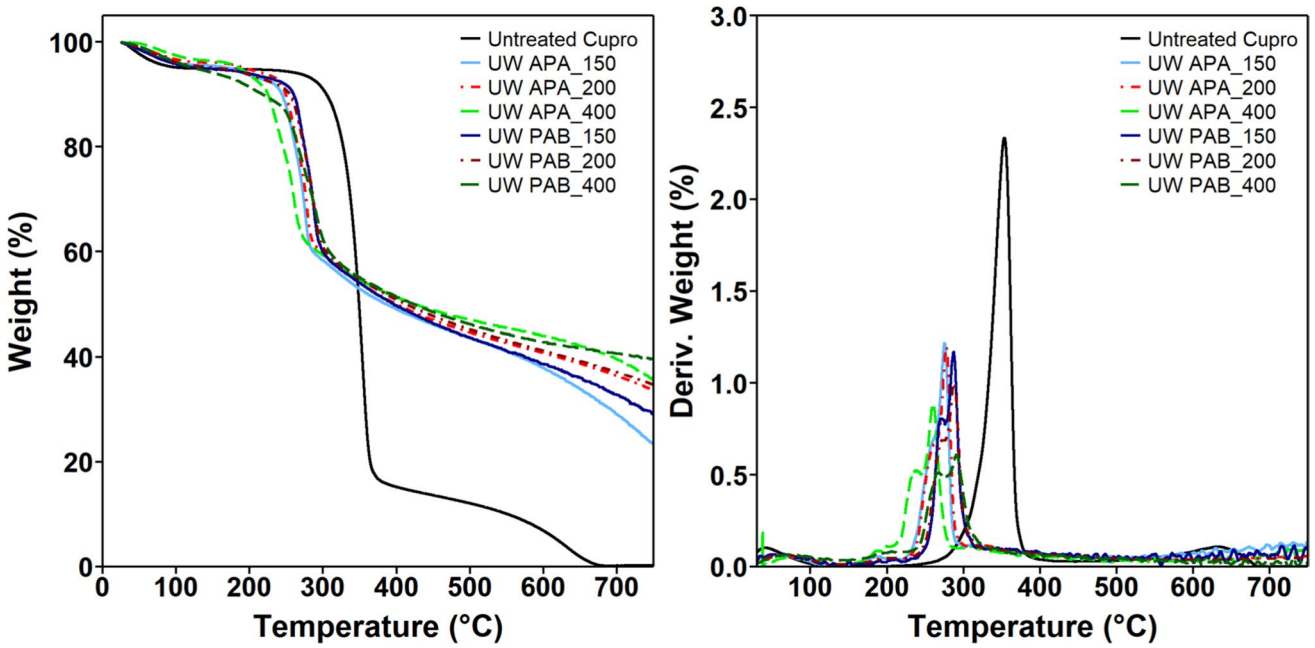

Fig. 9 TG and DTG curves of untreated cuprammonium fabric and unwashed APA/PAB-treated samples in nitrogen

enhanced char-forming ability. Among all the treated materials, those with a higher concentration (400 g/L) of FR materials showed the best performance, indicating a better coating during the functionalization process. Furthermore, the samples treated with PAB generally outperform the APA counterparts in terms of thermal resistance, with the UW PAB_400 achieving the highest final residue (40.63%).

As also shown in Table 4, most washed samples maintained a considerable level of thermal stability even after five washing cycles. This is evidenced by the T_5% and residue values, particularly for the 5W APA_400 sample, which exhibited a T_5% of 231.18 °C and a residue at 700 °C of 37.50%, indicating delayed mass loss and good char-forming ability. In comparison, the APA_200 sample showed reduced thermal stability, suggesting that a higher concentration of FR leads to a more durable and effective coating. On the other hand, PAB-treated samples showed a greater step decline in residues, with PAB_200 achieving only 0.11% after 5 washes. Moreover, at higher concentrations (400 g/L), APA_400 maintained more consistent residue across washes, while PAB_400 had a more significant reduction (to 25.79%). These findings indicate that, after washing, the APA treatments, especially at higher concentrations, retain superior thermal performance compared to their PAB-treated counterparts.

3.5 Mechanical Performance

Resistance to tearing is essential for ensuring durability and performance in applications where the material may be exposed to sharp edges, repeated stress, or harsh handling conditions. This is especially important for textiles used in protective gear or industrial applications. Untreated cuprammonium fabric showed a tear resistance of 9.84 cN alongside the warp and 15.65 cN alongside the weft. As demonstrated in Fig. 10, the incorporation of APA and PAB resulted in a decrease in tear strength in both the warp and weft directions, with the reduction being proportional to the FR concentration. In both cases, the reduction can be attributed to cellulose thermal degradation and acid hydrolysis that occur during the drying process. These conditions can cause cellulose fibers to undergo partial hydrolysis and oxidation, resulting in the breakdown of the polymer chains. Indeed, as the concentration of FR increased, the tear strength decreased [23]. Furthermore, APA-treated samples showed a greater tear strength reduction than the PAB-treated counterparts. The reason is related to boron acting as a stabilizer between the phytic acid and the cellulose structure [60, 61].

In terms of comfort and functionality, fabric stiffness can be a good indicator of how a textile will drape, conform to the body, and feel in handling [62, 63]. Untreated cuprammonium fabric demonstrated flexural rigidity of 5.84 ± 0.03 10^{-3} mg cm^{-1}. The addition of APA and PAB increased flexural rigidity with increasing solution concentration. Fabrics treated with 150 g/L, 200 g/L, and 400 g/L of APA showed a flexural rigidity increase of 51.9%, 138.7%, and 109.9%, respectively. Meanwhile, at equivalent concentrations, the fabrics treated with PAB exhibited a flexural rigidity increase of 20.9%, 39.4%, and 143.8%. Compared with ammonium phytate (APA) alone, incorporating boric acid

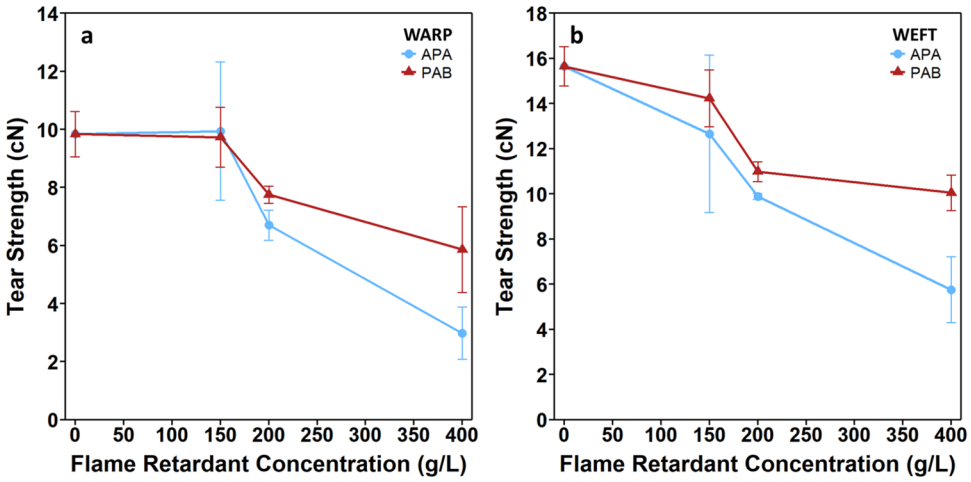

Fig. 10 Tear strength of unwashed APA-/PAB-treated samples according to flame-retardant concentration. The test was conducted in two directions: **a** along the warp and **b** along the weft

(PAB) increased bending length, likely due to the formation of a more rigid P–B–N finish layer structure. This reduces inter-fiber friction and stiffness, leading to enhanced fabric drapability and a shorter bending length. Findings are consistent with others P–B–N systems reported in the literature [33, 64].

3.6 Proposed Flame-Retardant Mechanism

For untreated cuprammonium fabric, dehydration and depolymerization occurred during combustion, with depolymerization being the dominant process. During this process, cellulose chains primarily degraded into levoglucosan, generating large amounts of volatile, flammable products, as shown in Fig. 11a. These included methane (2972, 2910, 2820, 2725 cm^{-1}), carbon monoxide (2180 cm^{-1}), aldehydes/ketones (1745 cm^{-1}), and alcohols (1121, 1065 cm^{-1}) [65, 66]. Moreover, it is also possible to observe strong peaks of carbon dioxide at 2355, 2320, and 650 cm^{-1} [67], indicating significant chain scission and oxidative decomposition.

After the functionalization with APA or PAB, the pyrolysis behavior of treated cuprammonium fabric was significantly altered, as shown by Fig. 11b and c. The cuprammonium fabric treated with APA at 400 g/L showed a clear reduction in volatile, flammable substances such as carbon monoxide (2180 and 2105 cm^{-1}), aldehydes/ketones (1715–1750 cm^{-1}), and alcohols (1070–1120 cm^{-1}), as well as the disappearance of peaks related to methane [68]. On

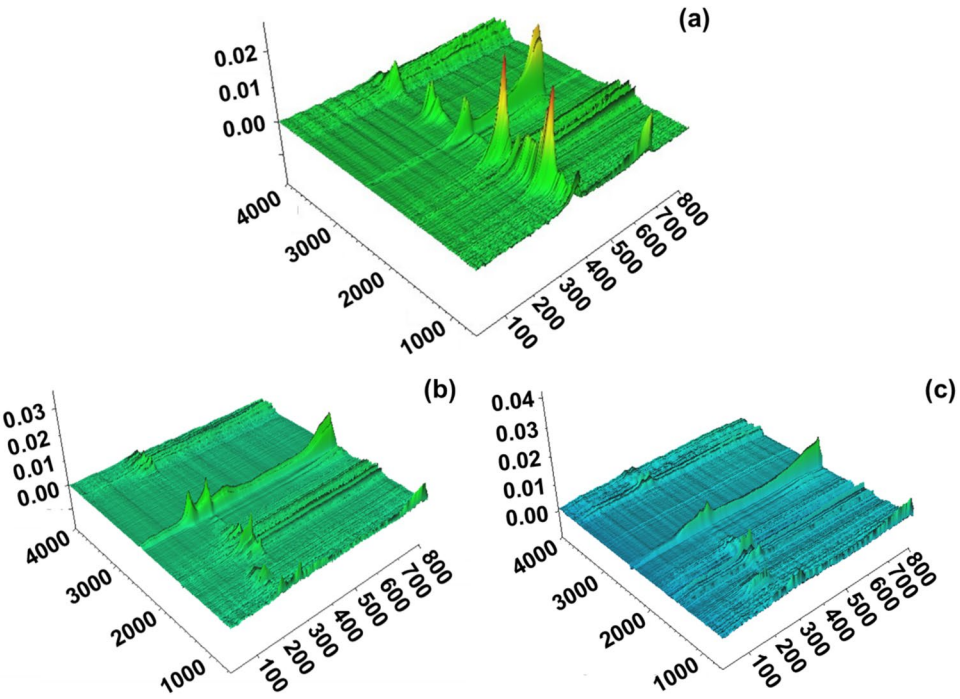

Fig. 11 Three-dimensional TG-FTIR spectra of: **a** untreated cuprammonium fabric, **b** APA_400, and **c** PAB_400

the other hand, nonflammable species including carbon dioxide (2359, 2321, 2310, 659 cm^{-1}) and water (3737, 3555, 1514 cm^{-1}) were released earlier and persisted throughout the degradation process [23, 69]. Moreover, two additional peaks at 959 and 931 cm^{-1} were observed, corresponding to NH_3 released from the ammonium groups of APA. Based on TG-FTIR analysis, the possible flame-retardant mechanism of APA is as follows: At high temperatures, the phosphoric molecules, covalently bound to the treated sample's backbone, undergoes acid-catalyzed scission, retarding the thermal decomposition process [68]. Meanwhile, the ammonium decomposed to release nonflammable gases (such as N_2 and NH_3), which create a barrier between the textile and oxygen, thereby extinguishing the flame. The APA thus works through a dual mechanism: gas-phase quenching by inert volatiles and condensed-phase protection via char reinforcement, with both effects arising synergistically from the combined presence of phosphorus and nitrogen. The observed decrease in ignitability and smoke production aligns with a dilution mechanism reported in similar P/N systems in the literature [23].

In the case of samples treated with PAB at 400 g/L (Fig. 11c), a mechanism like that of APA can be observed. The PAB-treated fabric also exhibited a significant reduction in the same volatile substances and the disappearance of methane. However, the overall peak intensities were lower than those of APA-treated samples, especially for carbon dioxide, suggesting more stable and continuous char formation. This effect can be attributed to the boron component, which undergoes multi-step dehydration and produces a thin, glass-like protective layer on the cellulose surface. Such a barrier not only enhances char yield but also contributes to reducing smoke release and toxic gas emissions during combustion [34, 59, 70].

4 Conclusions

Two eco-friendly flame-retardant materials, for imparting cuprammonium fabric with flame-retardant properties, were successfully investigated. Formulation APA consisted of phytic acid and urea, whereas formulation PAB additionally incorporated boric acid to exploit the P–B additive effect and enhance glassy-barrier formation during combustion. FTIR, SEM, and EDS analysis confirmed the successful functionalization of the cuprammonium fibers, where unwashed APA- and PAB-treated samples exhibited changes in their spectra bands, fiber morphology, and the presence of high values of N, P, and B. Furthermore, both systems demonstrated excellent flame-retardant properties, including self-extinguishing behavior and the formation of a strong char layer. Unwashed APA- and PAB-treated samples exhibited char lengths of 35 mm and 33 mm, respectively, during vertical flame testing, with corresponding residual weights of 39.54% and 40.63% at 700 °C. However, a noticeable difference in performance was observed after a few laundering cycles, where PAB-treated samples lost their flame-retardant properties, while APA-treated ones retained some part of them. Furthermore, SEM analysis of burned samples showed that PAB-treated samples had a more porous char layer. On the other hand, whiteness index analysis demonstrated that the incorporation of boron positively contributed to preserving the textile's whiteness, whereas APA-treated samples exhibited a noticeable brownish discoloration, with a CIE index of -19.9. The addition of boron also contributed to maintaining the textile's tear resistance, with PAB-treated samples exhibiting a tear strength of 5.86 cN in warp and 10.05 cN in weft compared to 2.98 cN and 5.76 cN, respectively, in the same directions of APA-treated samples. In summary, while both formulations imparted effective flame-retardant functionality to cuprammonium fabric, their trade-offs highlight complementary strengths, with APA offering superior washing durability and PAB enhancing mechanical and aesthetic properties.

Acknowledgements We would like to thank Dr Mariam Hadhri for helping with the experimental work and data collection.

Author Contributions All authors contributed to the study conception and design. Material preparation, data collection, and analysis were performed by Raphael P. Rosa. The first draft of the manuscript was written by Raphael P. Rosa and all authors commented on previous versions of the manuscript. All authors read and approved the final manuscript.

Funding Open access funding provided by Università degli Studi di Bergamo within the CRUI-CARE Agreement. The authors did not receive support from any organization for the submitted work.

Data availability The data that support the fi ndings of this study are available from the corresponding author, P. Rosa, R., uponreasonable request.

Declarations

Conflict of interest This is the original work of the author(s), and all the author(s) mutually agree that it should be submitted to Cellulose. All author(s) declared no potential conflicts of interest with respect to the research, authorship, and/or publication of this article.

References

1. K. Farhana, K. Kadirgama, A.S.F. Mahamude, M.T. Mica, Energy consumption, environmental impact, and implementation of renewable energy resources in global textile industries: An overview towards circularity and sustainability. Mater. Circ. Econ. **4**, 15 (2022). https://doi.org/10.1007/s42824-022-00059-1
2. Y. Zhang, X. Xia, K. Ma, G. Xia, M. Wu, Y.H. Cheung, H. Yu, B. Zou, X. Zhang, O.K. Farha et al., Functional textiles with smart properties: their fabrications and sustainable applications. Adv. Funct. Mater. (2023). https://doi.org/10.1002/adfm.202301607
3. E.O. Alegbe, T.O. Uthman, A review of history, properties, classification, applications and challenges of natural and synthetic dyes. Heliyon **10**, e33646 (2024). https://doi.org/10.1016/j.heliyon.2024.e33646
4. Maity, S.; Singha, K.; Pandit, P. 2023 Introduction to Functional and Technical Textiles. In *Functional and Technical Textiles*, (Elsevier, Amsterdam), p. 1–30.
5. Straits research textile market size, share & trends analysis report by raw material (cotton, chemical, wool, silk), by product (natural fibers, polyesters, nylon), by application (household, technical, fashion and clothing) and by region(North America, Europe, APAC, Midd Available online: https://straitsresearch.com/report/textile-market. Accessed 16 Jan 2025
6. Grand view research textile market size, share & trends analysis report by raw material (wool, chemical, silk), by product (natural fibers, polyester), by application, by region, and segment forecasts, 2024–2030; 2024
7. R.M. Frazier, M. Lendewig, R.E. Vera, K.A. Vivas, N. Forfora, I. Azuaje, A. Reynolds, R. Venditti, J.J. Pawlak, E. Ford et al., Textiles from non-wood feedstocks: Challenges and opportunities of current and emerging fiber spinning technologies. J. Bioresour. Bioprod. **9**, 410–432 (2024). https://doi.org/10.1016/j.jobab.2024.07.002
8. X. Chen, H.A. Memon, Y. Wang, I. Marriam, M. Tebyetekerwa, Circular economy and sustainability of the clothing and textile industry. Mater. Circ. Econ. **3**, 12 (2021). https://doi.org/10.1007/s42824-021-00026-2
9. S. Abbate, P. Centobelli, R. Cerchione, S.P. Nadeem, E. Riccio, Sustainability trends and gaps in the textile, apparel and fashion industries. Environ. Dev. Sustain. **26**, 2837–2864 (2023). https://doi.org/10.1007/s10668-022-02887-2
10. A.J. Sayyed, N.A. Deshmukh, D.V. Pinjari, A critical review of manufacturing processes used in regenerated cellulosic fibres: Viscose, cellulose acetate, cuprammonium, LiCl/DMAc, ionic liquids, and NMMO based lyocell. Cellulose **26**, 2913–2940 (2019). https://doi.org/10.1007/s10570-019-02318-y
11. Y. Liu, S. Ahmed, D.E. Sameen, Y. Wang, R. Lu, J. Dai, S. Li, W. Qin, A review of cellulose and its derivatives in biopolymer-based for food packaging application. Trends Food Sci. Technol. **112**, 532–546 (2021). https://doi.org/10.1016/j.tifs.2021.04.016
12. S. Wang, A. Lu, L. Zhang, Recent advances in regenerated cellulose materials. Prog. Polym. Sci. **53**, 169–206 (2016). https://doi.org/10.1016/j.progpolymsci.2015.07.003
13. X. Jiang, Y. Bai, X. Chen, W. Liu, A review on raw materials, commercial production and properties of Lyocell fiber. J. Bioresour. Bioprod. **5**, 16–25 (2020). https://doi.org/10.1016/j.jobab.2020.03.002
14. H. Shen, T. Sun, J. Zhou, Recent progress in regenerated cellulose fibers by wet spinning. Macromol. Mater. Eng. (2023). https://doi.org/10.1002/mame.202300089
15. P Parajuli S Acharya SS Rumi MT Hossain N Abidi, Regenerated cellulose in Textiles: Rayon, Lyocell, Modal and Other Fibres Elsevier In Fundamentals of Natural Fibres and Textiles 87–110 (2021)
16. A. Kasei, Care for people, care for earth, (2022)
17. I.S.F. Mendes, A. Prates, D.V. Evtuguin, Production of rayon fibres from cellulosic pulps: state of the art and current developments. Carbohydr. Polym. **273**, 118466 (2021). https://doi.org/10.1016/j.carbpol.2021.118466
18. S. Varnaitė-Žuravliova, J. Baltušnikaitė-Guzaitienė, Properties, production, and recycling of regenerated cellulose fibers: special medical applications. J. Funct. Biomater. **15**, 348 (2024). https://doi.org/10.3390/jfb15110348
19. X. Zhang, H. Zhang, D. Pan, W. Wu, H. Ma, J. Cao, J. Xu, The relationship between the structure and electrical properties of a cuprammonium filament via coated graphene. Pigment Resin Technol. **51**, 381–389 (2022). https://doi.org/10.1108/PRT-11-2019-0102
20. H.-W. Cui, K. Suganuma, H. Uchida, Highly stretchable, electrically conductive textiles fabricated from silver nanowires and cupro fabrics using a simple dipping-drying method. Nano Res. **8**, 1604–1614 (2015). https://doi.org/10.1007/s12274-014-0649-y
21. D. Iqbal, R. Ullah, M.I. Sarwar, R. Zhao, X. Ning, Fabrication and adsorption characteristics of cuprammonium cellulose-based membranes for removing anionic and cationic dyes. Colloids Surf A Physicochem Eng Asp **705**, 135692 (2025). https://doi.org/10.1016/j.colsurfa.2024.135692
22. M. Wang, G.-Z. Yin, Y. Yang, W. Fu, J.L. Díaz Palencia, J. Zhao, N. Wang, Y. Jiang, D.-Y. Wang, Bio-based flame retardants to polymers: a review. Adv. Ind. Eng. Polym. Res. **6**, 132–155 (2023). https://doi.org/10.1016/j.aiepr.2022.07.003
23. X. Liu, Q. Zhang, B. Cheng, Y. Ren, Y. Zhang, C. Ding, Durable flame retardant cellulosic fibers modified with novel, facile and efficient phytic acid-based finishing agent. Cellulose **25**, 799–811 (2018). https://doi.org/10.1007/s10570-017-1550-0
24. L. Costes, F. Laoutid, S. Brohez, P. Dubois, Bio-based flame retardants: when nature meets fire protection. Mater. Sci. Eng. R. Rep. **117**, 1–25 (2017). https://doi.org/10.1016/j.mser.2017.04.001
25. H. Hadi Alkarawi, G. Zotz, Phytic Acid in green leaves. Plant Biol. **16**, 697–701 (2014). https://doi.org/10.1111/plb.12136
26. T.C. Mokhena, E.R. Sadiku, S.S. Ray, M.J. Mochane, K.P. Matabola, M. Motloung, Flame retardancy efficacy of Phytic acid: an overview. J. Appl. Polym. Sci. (2022). https://doi.org/10.1002/app.52495
27. X.-W. Cheng, J.-P. Guan, R.-C. Tang, K.-Q. Liu, Phytic Acid as a bio-based phosphorus flame retardant for poly(lactic acid) nonwoven fabric. J. Clean. Prod. **124**, 114–119 (2016). https://doi.org/10.1016/j.jclepro.2016.02.113
28. B. Cromwell, A. Levenson, M. Levine, Thermogravimetric analysis of aromatic boronic acids for potential flame retardant applications. Thermochim. Acta **683**, 178476 (2020). https://doi.org/10.1016/j.tca.2019.178476
29. Y. Shi, L. Wang, M. Wu, Y. Wang, H. Li, An eco-friendly B/P/N flame retardant for its fabrication of high-effective and durable flame-retardant cotton fabric. Cellulose **30**, 6621–6638 (2023). https://doi.org/10.1007/s10570-023-05265-x
30. M.S. Özer, S. Gaan, Recent developments in phosphorus based flame retardant coatings for textiles: synthesis, applications and performance. Prog. Org. Coat. **171**, 107027 (2022). https://doi.org/10.1016/j.porgcoat.2022.107027
31. S.-Y. Lu, I. Hamerton, Recent developments in the chemistry of halogen-free flame retardant polymers. Prog. Polym. Sci. **27**, 1661–1712 (2002). https://doi.org/10.1016/S0079-6700(02)00018-7
32. V. Trovato, S. Sfameni, R. Ben Debabis, G. Rando, G. Rosace, G. Malucelli, M.R. Plutino, How to address flame-retardant technology on cotton fabrics by using functional inorganic sol–gel precursors and nanofillers: flammability insights, research advances, and

sustainability challenges. Inorganics **11**, 306 (2023). https://doi.org/10.3390/inorganics11070306
33. W. Zhu, M. Yang, H. Huang, Z. Dai, B. Cheng, S. Hao, A phytic acid-based chelating coordination embedding structure of phosphorus–boron–nitride synergistic flame retardant to enhance durability and flame retardancy of cotton. Cellulose **27**, 4817–4829 (2020). https://doi.org/10.1007/s10570-020-03063-3
34. W. Zhu, Q. Wang, M. Yang, M. Li, C. Zheng, D. Li, X. Zhang, B. Cheng, Z. Dai, Reactive flame-retardant cotton fabric coating: combustion behavior, durability, and enhanced retardant mechanism with ion transfer. Nanomaterials **12**, 4048 (2022). https://doi.org/10.3390/nano12224048
35. Y. Ma, X. Luo, L. Liu, C. Zhang, X. Shang, J. Yao, Eco-friendly, efficient and durable fireproof cotton fabric prepared by a feasible phytic acid grafting route. Cellulose **28**, 3887–3899 (2021). https://doi.org/10.1007/s10570-021-03767-0
36. J. Vasiljević, S. Hadžić, I. Jerman, L. Černe, B. Tomšič, J. Medved, M. Godec, B. Orel, B. Simončič, Study of flame-retardant finishing of cellulose fibres: organic-inorganic hybrid versus conventional organophosphonate. Polym. Degrad. Stab. **98**, 2602–2608 (2013). https://doi.org/10.1016/j.polymdegradstab.2013.09.020
37. J. Zhang, H. Huo, L. Zhang, Y. Yang, H. Li, Y. Ren, Z. Zhang, Effect of high-temperature hydrothermal treatment on the cellulose derived from the *Buxus* plant. Polymers **14**, 2053 (2022). https://doi.org/10.3390/polym14102053
38. ISO Textiles—Tests for colour fastness—Part C10: Colour fastness to washing with soap or soap and soda (2006)
39. ISO Textiles—Tests for colour fastness—Part J02: Instrumental assessment of relative whiteness. Int. Organ. Stand. (1997)
40. ISO Textiles—Tests for colour fastness—Part J03: Calculation of colour differences. Int. Organ. Stand. (2009)
41. Test method for flame resistance of textiles (Vertical Test) (2008)
42. Test method for tearing strength of fabrics by falling-pendulum (Elmendorf-Type) apparatus (2021)
43. Test method for stiffness of fabrics (2018)
44. V. Timón, B. Maté, V.J. Herrero, I. Tanarro, Infrared spectra of amorphous and crystalline urea ices. Phys. Chem. Chem. Phys. **23**, 22344–22351 (2021). https://doi.org/10.1039/D1CP03503G
45. C.K. Kundu, X. Wang, L. Song, Y. Hu, Borate cross-linked layer-by-layer assembly of green polyelectrolytes on polyamide 66 fabrics for flame-retardant treatment. Prog. Org. Coatings **121**, 173–181 (2018). https://doi.org/10.1016/j.porgcoat.2018.04.031
46. F. Xu, L. Zhong, C. Zhang, P. Wang, F. Zhang, G. Zhang, Novel high-efficiency casein-based P-N-containing flame retardants with multiple reactive groups for cotton fabrics. ACS Sustain. Chem. Eng. **7**, 13999–14008 (2019). https://doi.org/10.1021/acssuschemeng.9b02474
47. F. Safdar, M. Ashraf, A. Abid, A. Javid, K. Iqbal, Eco-friendly, efficient and durable flame retardant coating for cotton fabrics using phytic acid/silane hybrid sol. Mater. Chem. Phys. **311**, 128568 (2024). https://doi.org/10.1016/j.matchemphys.2023.128568
48. S.S. Hindi, Wastepaper-based cuprammonium rayon regenerated using novel gaseous–ammoniation injection process. Polymers **16**, 2431 (2024). https://doi.org/10.3390/polym16172431
49. W.J. Jones, W.J. Orville-Thomas, The infra-red spectrum and structure of dicyandiamide. Trans. Faraday Soc. **55**, 193 (1959). https://doi.org/10.1039/tf9595500193
50. X.-W. Cheng, J.-P. Guan, G. Chen, X.-H. Yang, R.-C. Tang, Adsorption and flame retardant properties of bio-based phytic acid on wool fabric. Polymers **8**, 122 (2016). https://doi.org/10.3390/polym8040122
51. K. Ahn, S. Zaccaron, N.S. Zwirchmayr, H. Hettegger, A. Hofinger, M. Bacher, U. Henniges, T. Hosoya, A. Potthast, T. Rosenau, Yellowing and brightness reversion of celluloses: CO or COOH, Who is the culprit? Cellulose **26**, 429–444 (2019). https://doi.org/10.1007/s10570-018-2200-x
52. H. Awada, D. Montplaisir, C. Daneault, The development of a composite based on cellulose fibres and polyvinyl alcohol in the presence of boric acid. BioResources **9**, 3439–3448 (2014)
53. M. Rietjens, P.A. Steenbergen, Crosslinking mechanism of boric acid with diols revisited. Eur. J. Inorg. Chem. **2005**, 1162–1174 (2005). https://doi.org/10.1002/ejic.200400674
54. W. Zhu, M. Yang, Q. Wang, X. Zhang, D. Li, Z. Xu, S. Liu, Z. Dai, An amino trimethylene phosphonic acid-based chelated boric acid complex that works as a synergistic flame retardant for enhancing the flame retardancy of cotton fabrics. J. Chin. Chem. Soc. **70**, 159–170 (2023). https://doi.org/10.1002/jccs.202200525
55. G. Rosace, C. Colleoni, V. Trovato, G. Iacono, G. Malucelli, Vinylphosphonic acid/methacrylamide system as a durable intumescent flame retardant for cotton fabric. Cellulose **24**, 3095–3108 (2017). https://doi.org/10.1007/s10570-017-1294-x
56. Y. Su, Z. Xu, M. Gao, Q. Zhao, X. Wang, F. Cheng, J. Shi, W. Wang, C. Cheng, Enhancing the flame retardancy of cellulose materials with phosphorylated MCA/lyocell blend fibre and synergistic flame retardancy mechanism. Cellulose (2025). https://doi.org/10.1007/s10570-025-06579-8
57. X. Liu, Y. Zhang, B. Cheng, Y. Ren, Q. Zhang, C. Ding, B. Peng, Preparation of durable and flame retardant lyocell fibers by a one-pot chemical treatment. Cellulose **25**, 6745–6758 (2018). https://doi.org/10.1007/s10570-018-2005-y
58. S. Li, F. Zhao, X. Wang, Z. Liu, J. Guo, Y. Li, S. Tan, Z. Xin, S. Zhao, L. Li, A green flame retardant coating based on one-step aqueous complexation of phytic acid and urea for fabrication of lightweight and high toughness flame retardant EPS insulation board. Polym. Degrad. Stab. **219**, 110597 (2024). https://doi.org/10.1016/j.polymdegradstab.2023.110597
59. M.N. Hassan, T.S. Abdullah, M.B. Mou, H.R. Towsif, Analysis of the flame retardancy effect of boron-containing compound on polyester-cotton blended fabric. Heliyon **10**, e34007 (2024). https://doi.org/10.1016/j.heliyon.2024.e34007
60. I. Stepina, A. Zhukov, S. Bazhenova, Modification of cellulosic materials with boron-nitrogen compounds. Polymers (Basel) **15**, 2788 (2023). https://doi.org/10.3390/polym15132788
61. H.T. Şahin, C. Bozkurt, M. Çiçekler, Investigating the effects of boron compounds on the cellulose fiber performance in paper recycling process. Chem. Pap. **78**, 4507–4516 (2024). https://doi.org/10.1007/s11696-024-03414-5
62. H. Sharifi, M. Vadood, A. Haji, Predicting the bending rigidity and formability of plasma-treated spunbond nonwoven fabrics using artificial intelligence. Text. Leather Rev. **7**, 1021–1038 (2024). https://doi.org/10.31881/TLR.2024.093
63. S. Ahmed, M.R. Repon, A.D. Pranta, A. Haji, J.Y. Al-Humaidi, M.M. Rahman, Performance analysis of functional properties of silk fabric enhanced via in situ grafting modification. Polym. Eng. Sci. **65**, 1474–1482 (2025). https://doi.org/10.1002/pen.27102
64. X. Liu, X. Jin, Y. Li, T. Zhang, W. Ni, Z. Lu, C. Dong, Bio-inspired "bionic armor" via P-B-N synergy and an alginate skeleton for superior flame-retardant polyester/cotton blends. Sustain. Mater. Technol. (2026). https://doi.org/10.1016/j.susmat.2026.e01915
65. S. Nam, B.D. Condon, Y. Liu, Q. He, Natural resistance of raw cotton fiber to heat evidenced by the suppressed depolymerization of cellulose. Polym. Degrad. Stab. **138**, 133–141 (2017). https://doi.org/10.1016/j.polymdegradstab.2017.03.005
66. P. Li, B. Wang, Y.-J. Xu, Z. Jiang, C. Dong, Y. Liu, P. Zhu, Eco-friendly flame-retardant cotton fabrics: preparation, flame retardancy, thermal degradation properties, and mechanism. ACS Sustain. Chem. Eng. **7**, 19246–19256 (2019). https://doi.org/10.1021/acssuschemeng.9b05523

67. B. Zheng, Y. Li, Q. Xie, Y. Gu, C. Wang, G. Chen, H. Li, The exploration of pyrolysis characteristics, kinetics and products of cotton via TG, FTIR, GC/MS and Shuffled Complex Evolution. J. Therm. Anal. Calorim. **149**, 14677–14686 (2024). https://doi.org/10.1007/s10973-024-13848-4
68. Q. Zhou, J. Chen, T. Zhou, J. Shao, In situ polymerization of polyaniline on cotton fabrics with Phytic Acid as a novel efficient dopant for flame retardancy and conductivity switching. New J. Chem. **44**, 3504–3513 (2020). https://doi.org/10.1039/C9NJ05689K
69. S. Huo, P. Song, B. Yu, S. Ran, V.S. Chevali, L. Liu, Z. Fang, H. Wang, Phosphorus-containing flame retardant epoxy thermosets: recent advances and future perspectives. Prog. Polym. Sci. **114**, 101366 (2021). https://doi.org/10.1016/j.progpolymsci.2021.101366
70. Y. Bai, J. Li, X. Tai, G. Wang, Preparation, characterization, and properties of novel Meglumine-based polysiloxane surfactants. J. Ind. Eng. Chem. **84**, 236–242 (2020). https://doi.org/10.1016/j.jiec.2020.01.003